Interfaces

How to cite:
International Edition: doi.org/10.1002/anie.202201392
German Edition: doi.org/10.1002/ange.202201392

In Situ Hydrolysis of Block Copolymers at the Water-Oil Interface

Zhan Chen, Mingqiu Hu, Xindi Li, Darren Smith, Hong-Gyu Seong, Todd Emrick, Javid Rzayev, and Thomas P. Russell**

Abstract: In situ manipulation of the chemical composition of block copolymers at the fluid interfaces affords a route by which the interfacial tension, the packing of the copolymers, and the penetration of the blocks into the two liquids can be manipulated. Here, a series of linear block copolymers of poly(solketal methacrylate-*b*-styrene) (PSM-*b*-PS) are used, converting hydrophobic PSM block into a hydrophilic glycerol monomethacrylate (GM) block, that results in a marked decrease in the liquid-liquid interfacial tension. The kinetics of the first-order hydrolysis reaction was analyzed by monitoring the time-dependent interfacial tension as a function of pH, polymer concentration, molecular weight, and composition. Fluorescence recovery after photobleaching (FRAP) was used to measure the in-plane dynamics of the copolymers before and after hydrolysis. Overall, this work provides insight into a quantitative pathway by which in situ interfacial reactions may be performed and monitored in real time, with complete alteration of the interfacial activity of the molecule.

Introduction

The self-assembly of block copolymers (BCPs) at liquid-liquid interfaces has been widely studied in emulsification,[1] droplet stabilization[2] and encapsulation.[3] Similar to traditional small molecules surfactants, amphiphilic BCPs can assemble at the water-oil interface with the hydrophobic and hydrophilic blocks solubilized in the oil and water phases, respectively, to minimize the interfacial energy. Controlling the interfacial assembly of BCPs involves manipulating the chemical functionality of the blocks to respond to external triggers or altering the chain architecture to impart specific properties to the assemblies.[1a,2a,c] For example, triblock copolymers with a crosslinkable mid-block, known as soft polymer Janus nanoparticles (NPs), can undergo configurational changes as the molecule approaches, and adsorbs to the interface to screen non-favorable interaction between the two immiscible liquids.[4] The spreading of the chains of these Janus NPs across the interface imparts a relaxation behavior to the assembly in response to expansion or contraction of the interfacial area. The responsiveness of copolymers assembled at the interface can also be made specific to changes in pH[5] or ionic strength,[6] or may be triggered by a conformational change due to exposure to light,[7] temperature[6c,7a] or chemical cues.[8] Here, we address a new concept in the interfacial assembly of block BCPs, where the chemical identity and amphiphilicity of the BCPs are completely changed in situ by converting an all hydrophobic BCP into a hydrophilic-hydrophobic BCPs by acid-catalyzed hydrolysis. Unlike previous studies where the amphiphilicity of the BCPs is unchanged significantly over the course of a reaction,[9] in this system, the random hydrolysis of one of the blocks leads to a marked changes in their interfacial behavior.

Recently, we described the synthesis and self-assembly of poly(solketal methacrylate)-*block*-polystyrene (PSM-*b*-PS).[10] These BCPs, having two hydrophobic blocks, can be converted into a hydrophilic-hydrophobic BCP by hydrolysis of the PSM block into poly(glycerol monomethacrylate) (PGM). The complete conversion increases the segmental interaction parameter χ by a factor of 13, from 0.035 to 0.438, switching the BCPs from a weakly to a strongly segregated regime. The hydrolysis was performed in dioxane solution catalyzed by hydrochloric acid (HCl) or in the solid state upon exposure to trifluoroacetic acid (TFA) vapor. The massive change in the nature of the BCPs brought about by this simple hydrolysis reaction makes PSM-*b*-PS an interesting material to probe the real-time, in situ evolution of BCP interfacial activity during the course of this transformation that can be monitored in real time and quantitatively by in situ dynamic pendant drop tensiometry. The interfacial tension provides direct, rapid information on the adsorption, assembly, and reaction of the BCPs at the interfaces, while the in-plane dynamics of the BCPs can be assessed by fluorescent recovery after photobleaching (FRAP),[11] providing a complete description of the BCPs during their interfacial hydrolysis.

Here, we describe the adsorption and hydrolysis of PSM-*b*-PS at the water-toluene interface by in situ pendant drop tensiometry, where the BCPs prior to hydrolysis were dissolved in toluene. Experiments were performed with a

[*] Z. Chen, M. Hu, H.-G. Seong, Prof. T. Emrick, Prof. T. P. Russell
Department of Polymer Science and Engineering,
University of Massachusetts
Amherst, MA 01003 (USA)
E-mail: russell@mail.pse.umass.edu
X. Li, D. Smith, Prof. J. Rzayev
Department of Chemistry, University at Buffalo,
The State University of New York
Buffalo, NY 14260-3000 (USA)
E-mail: jrzayev@buffalo.edu
Prof. T. P. Russell
Material Science Division, Lawrence Berkeley National Laboratory
Cyclotron Road, Berkeley, CA 94720 (USA)

pendant aqueous drop in a toluene solution of the BCPs and, in an inverted configuration, with a toluene drop of the BCPs in the aqueous phase. In the inverted configuration, the PSM-*b*-PS diffused and assembled at the water-toluene interface, then HCl was added to the water to trigger hydrolysis. We developed a model describing the hydrolysis kinetics and the corresponding change in the interfacial tension to determine the reaction rate constant with variation of polymer concentration, molecular weight, and composition (monomer volume fraction), and the pH of the aqueous phase. The in-plane diffusion coefficients of PSM-*b*-PS before and after hydrolysis were compared to the bulk solution diffusion coefficient. Along with ex situ hydrolysis measurements, we demonstrated that the water-oil interface provides a unique platform to perform chemical reactions in conjunction with responsive BCPs and smart structured liquids.

Results and Discussion

Three PSM-*b*-PS BCPs with different molecular weights and volume fractions, listed in Table 1, were synthesized by reversible addition-fragmentation chain-transfer (RAFT) polymerization, as detailed in previous publications.[10a–d] The number-average molecular weights of the synthesized copolymers were determined by ^{1}H NMR end-group analysis (Figure S1) while the relative molecular weights and dispersity ($Đ$) were estimated by gel permeation chromatography (GPC). Two fluorescently labelled copolymers were prepared by introducing 1 mol % of fluorescein-O-methacrylate segments into the PSM block.[12] Before hydrolysis, both blocks of PSM-*b*-PS are hydrophobic, and soluble in toluene without micelle formation. Using a J-shaped needle, the PSM-*b*-PS solution in toluene was injected into water phase (Figure 1a). After the assembly of PSM-*b*-PS at the water-oil interface equilibrated, HCl was introduced into the aqueous phase with gentle stirring, and the time dependence of the interfacial tension (γ) was measured to monitor the hydrolysis reaction of the PSM block and the subsequent reconfiguration of the copolymer at the interface. Figure 1b indicates that prior to adding the HCl into the water phase, P(SM2-S4) was interfacially active at the water-oil interface, since PSM is more polar than PS, with a preferential affinity to the water phase, while PS remains solubilized in the toluene phase. γ was observed to decrease as PSM-*b*-PS diffused to and assembled at the interface, plateauing after 1.5 h at 13.3 mN m^{-1}. Sufficient HCl was then added to the aqueous phase with gentle stirring to achieve 0.1 M HCl concentration. Upon addition of acid, γ decreased further, generating a random copolymer P(SM-*r*-GM) where the fraction of GM mers increases as a function of time until the entire block is hydrolyzed. After full conversion, γ= 8.1 mN m^{-1}.

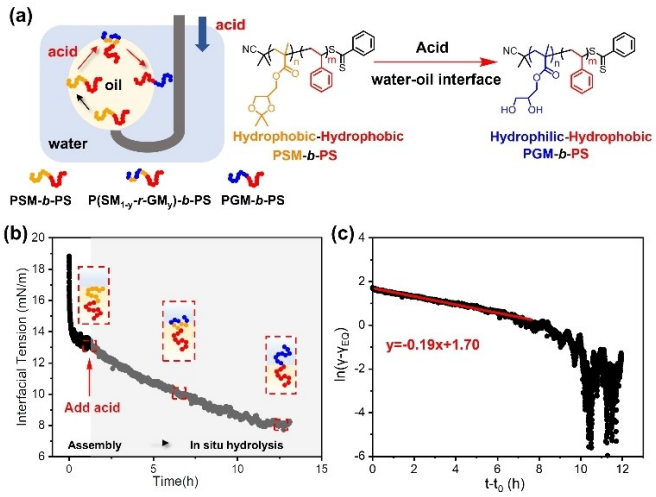

Figure 1. In situ hydrolysis of PSM-*b*-PS to PGM-*b*-PS at the water-oil interface in J-shape geometry. a) Scheme of the experimental setup and the hydrolysis reaction; b) Time evolution of interfacial tension of 1 mg mL^{-1} P(SM2-S4). After equilibration (1.5 h), HCl was added to the water phase with gentle stirring to make 0.1 M HCl solution (arrow in the figure); c) Linear fitting of (b) using equation $\ln(\gamma-\gamma_{EQ}) = \ln[N(\Delta E_1 - \Delta E_2)/A] - k(t-t_0)$ to calculate the in situ hydrolysis kinetics, where γ is the interfacial tension, γ_{EQ} is the equilibrium interfacial tension after adding acid, N/A is the BCP density at the water-oil interface, ΔE is the energy release due to adsorption of a polymer chain to the interface, subscripts 1 and 2 represent PSM-*b*-PS (before hydrolysis) and PGM-*b*-PS (fully converted), k is reaction rate constant, t is time, and t_0 is the time of acid addition.

To probe the reaction kinetics at the interface, we developed a model to calculate the interfacial hydrolysis rate constant from interfacial tension results.[13] For an interface with an area A and N adsorbed PSM-*b*-PS chains, the total energy at the water-oil interface can be expressed as:

$$E_I = \gamma_0 A + N\Delta E \quad (1)$$

Table 1: Characteristics of PSM-b-PS copolymer samples.

Code	PS block M_n [g mol^{-1}]	PSM block M_n [g mol^{-1}][a]	Total M_n [g mol^{-1}]	f_{PS}[b]	$Đ$[c]
P(SM2-S4)	4200	2200	6400	0.68	1.06
P(SM3-S4)	3700	3000	6700	0.58	1.12
P(SM4-S5)	5400	4400	9800	0.58	1.01
F-P(SM5-S5)[d]	5100	4800	9900	0.54	1.15
F-P(SM5-S7)[d]	7100	4800	11 900	0.62	1.14

[a] Calculated from ^{1}H NMR end group analysis. [b] Volume fraction of polystyrene block. [c] Determined by gel permeation chromatography (GPC) in tetrahydrofuran using PS calibration. [d] Dye-labeled F-PSM-*b*-PS is prepared by copolymerizing fluorescein O-methacrylate with the PSM at 0.1 molar ratio.

where γ_0 is the pure water-oil interfacial tension and ΔE is the energy decrease due to the adsorption of a single polymer to the interface. Assuming that the hydrolysis occurs randomly along the PSM chain contacting aqueous phase and homogeneously across the water-oil interface, and that the reaction is first order (reasonable for this hydrolysis[14]), then ΔE for PSM-*b*-PS undergoing in situ hydrolysis to PGM-*b*-PS can be written as:

$$\Delta E = \Delta E_1 e^{-k(t-t_0)} + \Delta E_2(1 - e^{-k(t-t_0)}) \quad (2)$$

where t_0 is taken as the time when HCl is added to the aqueous phase, k is the reaction rate constant, and subscripts 1 and 2 represent PSM-*b*-PS (before hydrolysis) and PGM-*b*-PS (fully converted), respectively. If the interfacial area is increased to $2A$, while preserving the total number of BCPs and density of the adsorbed BCPs, the interfacial energy can be expressed as:

$$E_{II} = 2\gamma_0 A + 2N\Delta E \quad (3)$$

From the definition of interface tension, γ can be written as:

$$\gamma = (E_{II} - E_I)/A = \gamma_0 + N\left[\Delta E_2 + (\Delta E_1 - \Delta E_2)e^{-k((t-t_0)}\right]/A \quad (4)$$

When the in situ hydrolysis is completed,

$$\gamma_{EQ} = \gamma_0 + N\Delta E_2/A \quad (5)$$

and γ_{EQ} is experimentally determined as equilibrium interfacial tension. By combining Equation (5) and (4).

$$\ln(\gamma - \gamma_{EQ}) = \ln[N(\Delta E_1 - \Delta E_2)/A] - k(t-t_0) \quad (6)$$

Using Equation (6), the in situ hydrolysis rate for 1 mg mL^{-1} solution of P(SM2-S4) at the water-oil interface against 0.1 M HCl in water is found to be 0.19 h^{-1}, as shown in Figure 1c. It should be noted that the deviation of experimental data from the linear fit at long times is thought to arise from the increased packing density due to the greater extension of the PGM into the aqueous phase than the starting PSM block.

A distinctly different behavior was observed when the experiments were performed in the classic pendant drop geometry where a 0.1 M HCl droplet was hung from the needle upon injection (I-geometry) into a toluene solution of PSM-*b*-PS, as shown in Figure 2a. In a control experiment, where a water droplet is injected into a toluene solution of PSM-*b*-PS, γ rapidly decreases and plateaus at an equilibrium γ of 14.0 mN m^{-1}, reflecting the diffusion and assembly of the PSM-*b*-PS at the water-oil interface. However, when the droplet consisted of aqueous acid (0.1 M HCl), the equilibrium interfacial tension is ≈3 mN m^{-1}, much lower than the 8 mN m^{-1} measured in the J-shape geometry. The evolution of interfacial tension in I-shape geometry can be divided into two regimes when plotted on a semi-log scale (Figure S5). Since the PSM-*b*-PS immediately undergoes in situ hydrolysis after adsorption to the interface, the first regime is, therefore, a mixed-mode of assembly and hydrolysis. In contrast in the J-shape geometry, assembly and hydrolysis are in separate regimes, due to the different pathways used for introducing acid. The second regime in the I-shape geometry, beginning after 16 h of incubation, decreased the interfacial tension from 5.5 mN m^{-1} to 3.0 mN m^{-1}, and was consistently observed for different acid concentrations, which may be due to reconfiguration of PGM-*b*-PS. The interfacial assemblies at different times were transferred to silicon wafers (excess PSM-*b*-PS in the oil phase was removed by an exhaustive replacement of the oil phase with pure oil prior to transfer (Figure S6)). As shown in Figure S7, the transferred interfacial assembly formed a hole-island morphology after drying, as evidenced by atomic force microscopy (AFM) analysis, as would be

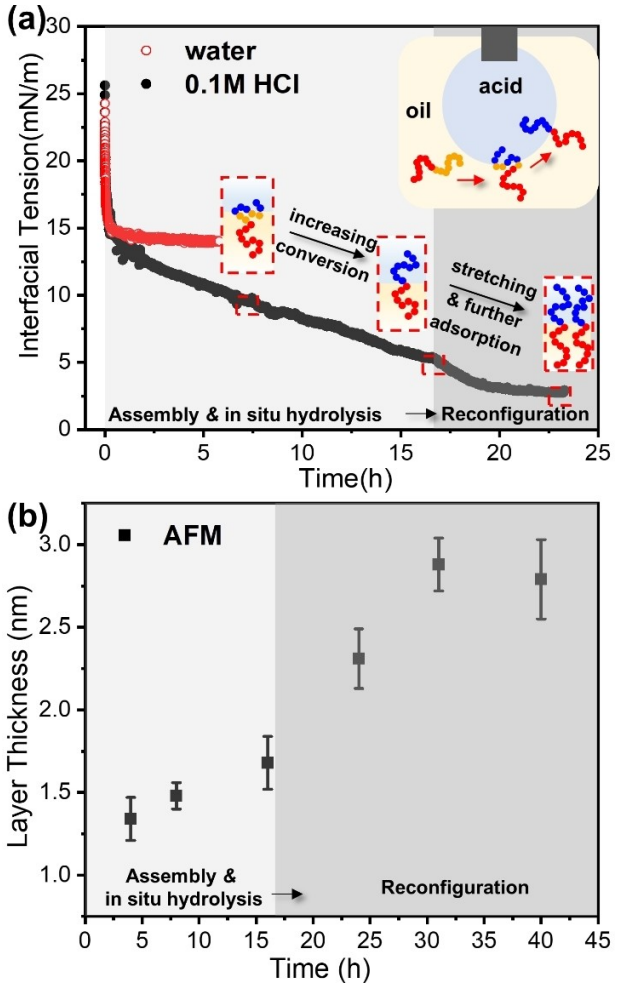

Figure 2. In situ hydrolysis of PSM-*b*-PS to PGM-*b*-PS at the water-oil interface in I-shape geometry. a) Time evolution of interfacial tension of 1 mg mL^{-1} P(SM2-S4) at the water-oil interface with a water or a 0.1 M HCl (aq) droplet; b) Transferred layer thickness of 1 mg mL^{-1} P(SM4-S2) between the ater-oil interface (0.1 M HCl in water phase) at different aging times, measured by AFM (The results were averaged by repeating experiments 3 times and each experiment was taken 3 images).

expected for thin diblock copolymer films.[15] The depressed areas, or holes, correspond to bare silicon substrate, while the islands are the interfacial assemblies that have formed lamellar domains oriented parallel to the substrate. The step height for different islands in same image are the same and can be explained as single molecule layer, the size of which is in keeping with the SAXS results (Figure S8), as would be expected. The product of step height and the fractional areal coverage (referred as layer thickness) is proportional to the thickness of the copolymer interfacial assembly, the number of copolymer chains at the interface, and the areal density of chains at the interface as a function of time. Repeated experiments yielded the reported statistical averages. The results in Figure 2b show that layer thickness increased gradually with assembly and hydrolysis, and then at ≈17 h, an acceleration in the number of copolymer chains at the interface plateau after ≈30 h. This change maps onto the interfacial tension results where the γ is seen to gradually decrease up to ≈17 h, then changes abruptly to an equilibrium value of ≈3 mN m^{-1}.

Increasing the conversion of PSM to PGM during hydrolysis increases the solvation of PGM in the water phase, and likely extends the PGM block into the aqueous phase, maximizing favorable PGM-water contacts. Since the "surfactancy" of the copolymer increases with hydrolysis, a reduction in γ would be expected with a polymer adsorption at the interface. With increasing extension of the hydrolyzed PSM block into the aqueous phase, there is an increasing mismatch of the projection of the PSM and PS blocks onto the interface since there is no driving force to stretch the PS block. This mismatch would drive the system away from planarity, envisaged of an interface bent towards the hydrolyzing block. The further drop in γ and the acceleration in copolymers adsorption at the interface indicates a change in the nature of the assembly at the interface. The conversion of PSM to a PGM increases the surfactancy of the copolymer, so that more copolymers adsorb to the interface and, rather than bending the interface, the PS block begins to stretch, decreasing the projection of the PS block onto the interface. Consequently, the increased packing density of the copolymer chains at the interface gives rise to a reconfiguration of the PS block. The reconfiguration regime in I-shape geometry is more evident than in J-shape. We attribute the difference to (1) the surrounding oil medium in the I-shape geometry providing an opportunity for more BCPs to adsorb; (2) the simultaneous assembly and in situ hydrolysis in the I-shape geometry is different from the sequential assembly and hydrolysis in the J-shape geometry. The binding energy of BCPs is not high enough to hold the BCPs at the interface when the droplet volume is reduced, as shown in Figure S9, in comparison to the much stronger binding energy of NP-surfactants, where wrinkles are seen when droplet volume is reduced.[4]

The interfacial activity of PSM-*b*-PS was further changed by adjusting the pH and polymer concentration. Figure 3a shows interfacial tension results of 1 mg mL^{-1} solutions of PSM-*b*-PS in toluene against water with different concentrations of HCl added to the aqueous phase after 1.5 h adsorption of the PSM-*b*-PS to the interface (indicated by the arrow in the figure). At constant BCP concentration and increasing acid concentration, the in situ hydrolysis accelerated with rate constants (calculated from the slope of $\ln(\gamma - \gamma_{EQ})$vs. $t - t_0$ (Figure 3b)) found to be 0.056 h^{-1}, 0.19 h^{-1}, and 3.48 h^{-1} for 0.01 M, 0.1 M and 1 M HCl concentrations, respectively. The sudden drop in the γ after adding 1 M HCl arises from a pause in the measurement to allow for 1 min stirring and significant interfacial energy change. Figure 3c shows the interfacial tension as a function of time for different PSM-*b*-PS concentrations at 0.1 M HCl. As can be seen, increasing the concentration of PSM-*b*-PS reduces the equilibrium γ before and after hydrolysis due to an increase in the polymer packing density. The hydrolysis rate was found to be slightly dependent on the PSM-*b*-PS concentration, with rate constants (calculated from Figure 3d) of 0.21 h^{-1}, 0.19 h^{-1}, and 0.17 h^{-1} for 0.01 mg mL^{-1}, 1 mg mL^{-1}, and 10 mg mL^{-1} PSM-*b*-PS concentrations (specifically P(SM2-S4)). The results indicate that higher packing density at the interface will only slightly reduces reaction rate, reflecting a slightly slower penetration of the acid into the densely packed PSM blocks.

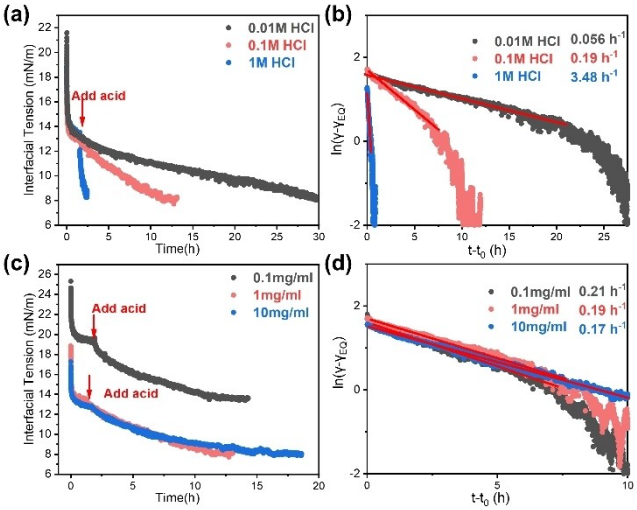

Figure 3. Varying in situ hydrolysis conditions for P(SM2-S4) at the water-oil interface in a J-shape geometry. a) Time evolution of interfacial tension, and b) the corresponding linear fitting to calculate the in situ hydrolysis kinetics, of 1 mg mL^{-1} P(SM2-S4) with different HCl concentrations in the aqueous phase. c) Time evolution of interfacial tension, and d) the corresponding linear fitting to calculate the in situ hydrolysis kinetics of different P(SM2-S4) concentration with 0.1 M HCl in aqueous phase. After the assembly of P(SM2-S4) at the water-oil interface equilibrated (1.5 h aging), HCl was introduced into the aqueous phase with gentle stirring, as indicated by the arrow in the figures.

The Janus interfacial conformation of PSM-*b*-PS at the water-oil interface was also changed by varying the volume fraction of the blocks in the copolymer and the molecular weight. Before adding acid, the interfacial tension as a function of time for three different PSM-*b*-PS copolymers is shown in Figure 4a (inset). P(SM2-S4) with a molecular weight similar to P(SM3-S4), but a more asymmetric composition, showed higher γ. P(SM4-S5) with a similar volume fraction as P(SM3-S4), but higher molecular

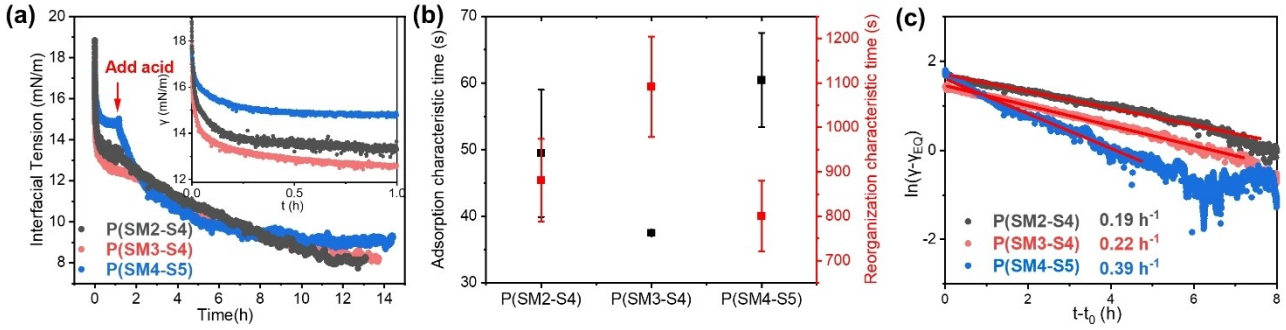

Figure 4. PSM-*b*-PS with different molecular weights and volume fractions at the water-oil interface in J-shape geometry. a) Time evolution of interfacial tension for 1 mg mL^{-1} of PSM-*b*-PS at the water-oil interface in J-shape geometry. After the assembly of PSM-*b*-PS at the water-oil interface equilibrated (1.5 h aging), HCl (aq) was introduced into the aqueous phase with gentle stirring to make a 0.1 M HCl solution, as indicated by the arrow. The inset figure is the zoom-in region before acid was added; b) Adsorption and reorganization characteristic times of 1 mg mL^{-1} of PSM-*b*-PS at the water-oil interface, calculated from (a) before adding acid with equation $\gamma = Ae^{-t/\tau_{\text{adsorption}}} + Be^{-t/\tau_{\text{reorganization}}} + C$. The results are averaged by repeating experiments; c) Linear fitting of (a) to calculate the in situ hydrolysis kinetic.

weight, also exhibited a higher γ value, due to a lower molar concentration of P(SM3-S4) in the oil droplet. The decrease in γ as a function of time arises from the adsorption and reorganization of PSM-*b*-PS chains at the interface, which can be described by two distinct relaxations: the adsorption of PSM-*b*-PS to interface with a characteristic relaxation time of $\tau_{\text{adsorption}}$ and the reorganization of copolymers that combines the in-plane assembly of BCPs at the interface and further adsorption with a characteristic relaxation time of $\tau_{\text{reorganization}}$.

$$\gamma = Ae^{-t/\tau_{\text{adsorption}}} + Be^{-t/\tau_{\text{reorganization}}} + C \tag{7}$$

As shown in Figure S10 and Figure 4b, the characteristic adsorption and reorganization times for three PSM-*b*-PS samples are calculated from Equation (7), where the reorganization time is two orders of magnitude longer than the adsorption time, indicating that reorganization at the interface is a coordinated motion of multiple chains, while the initial adsorption is a more rapid, single chain process. P(SM4-S5) with a higher molecular weight has a longer characteristic time for adsorption, but a shorter time for reorganization in comparison to P(SM3-S4), indicating that the diffusion and adsorption of P(SM3-S4) are more rapid with more efficient chain packing at the interface, giving rise to longer reorganization relaxation times. P(SM2-S4), with a molecular weight similar to P(SM3-S4), but more asymmetric in composition, has a longer characteristic time for adsorption, but a shorter reorganization relaxation time, suggesting that greater chain entanglement on either side of the interface for the more symmetric molecule.

Having studied the interfacial behaviors before conversion, we then sought to understand the response of those molecules during in situ hydrolysis. With 0.1 M HCl in the aqueous phase, the in situ hydrolysis rate constant varied as follows: 0.19 h^{-1}, 0.22 h^{-1}, 0.39 h^{-1} for P(SM2-S4), P(SM3-S4) and P(SM4-S5), respectively (Figure 4c). It was observed that P(SM4-S5) has a considerably larger reaction rate than P(SM3-4). Mechanisms by which this might occur include: (1) The equilibrium interfacial tension of P(SM4-S5) is notably greater than that of P(SM3-S4) (15 mN m^{-1} against 12 mN m^{-1}), resulting in a loosely packed interface that enables easy penetration of the acid into the inner PSM blocks; and (2) P(SM4-S5) with a larger PSM block volume has higher projected area onto the interface, giving more access of acid to PSM blocks. In the context of volume ratio studies, PSM is more crowded at the interface for smaller PSM volume ratios, which will relatively lower its exposure to acid, explaining why P(SM2-S4) has a slightly smaller reaction rate constant than P(SM3-S4).

The equilibrium in-plane dynamics of the copolymer assemblies at the interface was investigated by fluorescence recovery after photobleaching (FRAP). Two different fluorescent F-PSM-*b*-PS copolymers were prepared by copolymerization of SM with fluorescein-O-methacrylate, followed by polymerizing different lengths of PS, as evidenced by ^{1}H NMR, GPC and fluorescence spectrometry (Figure S2–S4).[12] As shown in Figure 5a, γ values of the two F-PSM-*b*-PS decrease initially due to the interfacial assembly, and are further diminished upon the addition of acid due to in situ hydrolysis. The γ of F-P(SM5-S7) is slightly lower than that of F-P(SM5-S5), since it is more symmetric in composition before and after conversion. Both copolymers showed similar characteristic adsorption and reorganization times (Figure S11, Figure 5b) and had similar in situ hydrolysis rates, as shown in Figure 5c. FRAP experiments were performed on the equilibrated assemblies before and after hydrolysis. As shown in the insets of Figure 5d–g, the fluorescence ring confirms that the copolymer preferentially locates at the water-oil interface. After photobleaching, the fluorescence recovery was evident, where the normalized recovery of intensity followed:

$$Intensity = A\left(1 - e^{-t/\tau_{\text{in-plane diffusion}}}\right) \tag{8}$$

The resulting characteristic time $\tau_{\text{in-plane diffusion}}$ is used to calculate the in-plane diffusion coefficient by

$$D = \omega^2/4\tau_{\text{in-plane diffusion}} \tag{9}$$

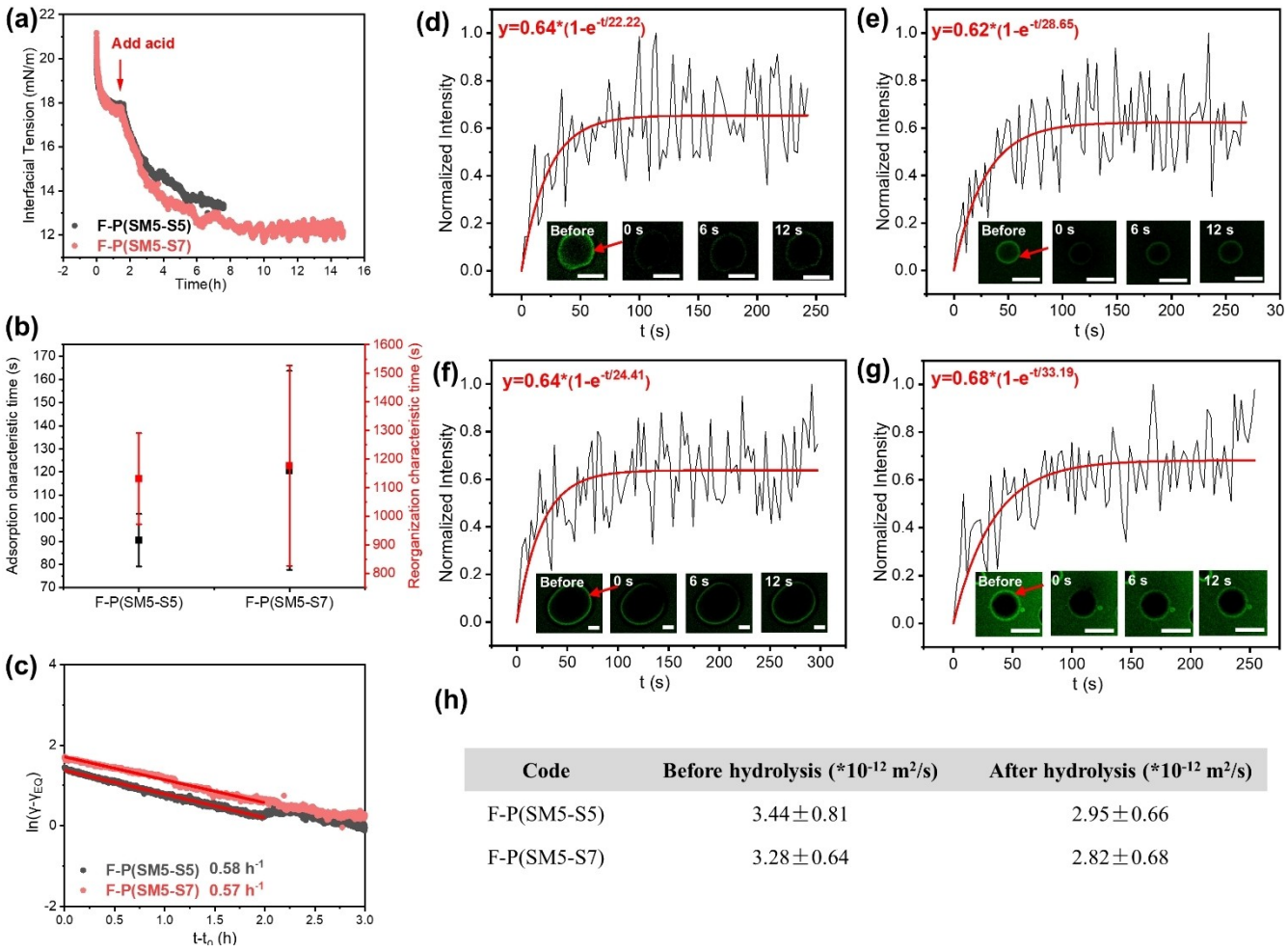

Code	Before hydrolysis (*10^{-12} m^2/s)	After hydrolysis (*10^{-12} m^2/s)
F-P(SM5-S5)	3.44±0.81	2.95±0.66
F-P(SM5-S7)	3.28±0.64	2.82±0.68

Figure 5. Fluorescent F-PSM-*b*-PS characterization by pendant drop tensiometry and FRAP. a) 1 mg mL^{-1} F-PSM-*b*-PS at the water-oil interface and in situ hydrolysis with 0.1 M HCl after 1.5 h aging. b) Adsorption and reorganization characteristic time for 1 mg mL^{-1} of F-PSM-*b*-PS at the water-oil interface, calculated from (a) before adding acid. The results are averaged by repeating experiments. c) Linear fitting of (a) to calculate the in situ hydrolysis kinetics. FRAP for F-P(SM5-S5) before hydrolysis (d), after hydrolysis (e), F-P(SM5-S7) before hydrolysis (f), and after hydrolysis (h). NaOH was added to water phase to reach 0.5 mM with 1 mg mL^{-1} F-PSM-*b*-PS in toluene in (d) and (f). 0.1 M HCl-toluene emulsion, with 1 mg mL^{-1} F-PSM-*b*-PS dissolved in toluene phase, was prepared for converting F-PSM-*b*-PS into F-PGM-*b*-PS overnight then NaOH solution was added to neutralize the aqueous phase in (e) and (g). The emulsion droplet was point-bleached as arrow indicated inside figure. The normalized fluorescence intensity was fit by the relaxation equation: $Intensity = A\left(1 - e^{-t/\tau_{\text{in-plane diffusion}}}\right)$. Scale bar: 200 μm. h) The summarized in-plane diffusion coefficients before and after hydrolysis.

where ω is the radius of the focused beam. By photobleaching a spin-coated F-PSM-*b*-PS film under the identical conditions and camera settings, ω was determined to be 17.4 mm (Figure S12). We note that 0.5 mM NaOH aqueous solution was prepared as water phase to increase the fluorescence yield before the conversion studies, while a 0.1 M HCl-toluene emulsion was prepared and incubated overnight to convert F-PSM-*b*-PS into F-PGM-*b*-PS, then an equivalent molar NaOH solution was added to neutralize the aqueous phase for same purpose (Figure S13).[16] The calculated in-plane diffusion coefficients are summarized in Figure 5h, which shows the in-plane diffusion coefficient after hydrolysis to be slightly lower than before hydrolysis, reflecting the higher packing density of the interface after the in situ hydrolysis. Both copolymers showed similar in-plane diffusion coefficients before and after hydrolysis, since the molecular weights and chemical structures are similar. The bulk diffusion coefficient of F-PSM-*b*-PS in toluene was estimated to be 5×10^{-11} m^2s^{-1} from P(SM13-S14), since the molecular weight of F-PSM-*b*-PS is too low for measurement by DLS (Figure S14). This is an order of magnitude greater than the in-plane diffusion coefficient evaluated by FRAP.

Experiments were also performed where the hydrolysis was first done ex situ, i.e., in solution, for different times, converting the PSM block into a random copolymer of P(SM_{1-y}-*r*-GM_y), where *y*, the fraction of GM, increased with increasing ex situ hydrolysis time (Figure S15). The degree of conversion was measured by ^{1}H NMR spectroscopy, where the ratio of the peak areas of the hydroxy group in GM segments and the methyl group in the backbone was calculated. For 100 % conversion, this ratio

was scaled to unity. P(SM_{1-y}-*r*-GM_y)-*b*-PS was freeze dried and redissolved in toluene, and the interfacial tension was then measured against pure water. The equilibrium interfacial tension decreased, as the fraction of GM units increased, but for $y > 0.45$ the interfacial tension continually increased. This result, at first glance, is surprising, since the hydrophilicity of the P(SM-*r*-GM) block increases and one would expect the interfacial tension to continuously decrease. However, it is apparent from the DLS measurements (Figure S16) that the hydrolyzed copolymers undergo aggregation in the toluene phase, with micelle sizes increasing with *y*, leaving fewer free chains to adsorb to the droplet interface and giving rise to the observed increase in the interfacial tension. It is also important to note that with the pendant drop experiments, there is an additional air/toluene interfacial area that is much larger than the droplet interface that competes for free copolymer chains. Additionally, for the copolymers to adsorb to either the air/toluene surface or the water/toluene interface, the micelles would need to be disrupted at the interface, which would necessitate the disruption of strong hydrogen bonding between the GM units.[10c]

Conclusion

In conclusion, the kinetics of the in situ hydrolysis of PSM-*b*-PS assembled at the water-oil interface were determined by the time-dependent decrease in the interfacial tension. Using a J-shape needle, a droplet containing solution of PSM-*b*-PS in toluene was introduced to a water phase. After the adsorption and assembly of PSM-*b*-PS equilibrated, conversion of the PSM-*b*-PS to P(SM_{1-y}-*r*-GM_y)$_n$, increased the hydrophilicity of the SM block and the binding energy of the copolymer to the interface. Experiments performed in the normal, I-shaped geometry led to a simultaneous adsorption and in situ hydrolysis at the interface, prohibiting assessment of the reaction kinetics. Lower equilibrium interfacial tension was found in I-shape due to more evident in-plane reconfiguration, seen as a sudden drop in the interfacial tension that reflects a rapid increase in the amount of copolymer adsorbed to the interface. The in situ hydrolysis reaction kinetics was altered by varying the polymer and acid concentration, referring to tuning packing density and catalyst amount. The in situ hydrolysis rate constant would increase with increasing catalyst amount or decreasing packing density. The molecular weight and composition (monomer volume fraction) were varied to investigate the influence on adsorption, assembly, and in situ hydrolysis kinetics at the water-oil interface. Prior to hydrolysis reaction, characteristic relaxation times for adsorption and reorganization were determined from the change in the interfacial tension, where P(SM3-S4) with smaller molecular weight and symmetric volume composition has smaller characteristic adsorption time but higher reorganization time compared to P(SM4-S5) and P(SM2-S4), respectively. In context of in situ hydrolysis kinetics, the reaction rate constant of P(SM3-S4) is much smaller than P(SM4-S5) due to the more densely packed interface and smaller projection area of SM at interface, both decreasing the area of the interface exposed to the aqueous phase, whereas P(SM2-S4) has smaller in situ hydrolysis rate than P(SM3-S4) because the asymmetric composition leads to PSM being more crowded at the water-oil interface and a reduced penetration of the aqueous phase. FRAP was used to determine the in-plane diffusion coefficient, which was one order of magnitude lower than that in the bulk solution and has a smaller value after hydrolysis. Given with ex situ hydrolysis results, we believe that the water-oil interface provides a unique platform to perform chemical reactions for the design of responsive BCPs for smart structured liquids with tailored interfacial energy.

Acknowledgements

This material is based upon work supported by the Air Force Office of Scientific Research under award number FA9550-21-1-0388 and by the Army Research Office under Contract No. W911NF-20-0093. We also thank Dr. James Chambers for helpful discussions of FRAP experiments. The fluorescence microscopy data was collected in the Light Microscopy Facility and Nikon Center of Excellence at the Institute for Applied Life Sciences (IALS) at UMass Amherst, with support from the Massachusetts Life Sciences Center.

Conflict of Interest

The authors declare no conflict of interest.

Data Availability Statement

The data that support the findings of this study are available from the corresponding author upon reasonable request.

Keywords: Block Copolymers · In Situ Hydrolysis · Interfaces · Reconfiguration · Self-Assembly

[1] a) M. Hu, T. P. Russell, *Mater. Chem. Front.* **2021**, *5*, 1205–1220; b) P. S. Clegg, J. W. Tavacoli, P. J. Wilde, *Soft Matter* **2016**, *12*, 998–1008.

[2] a) G. Xie, P. Krys, R. D. Tilton, K. Matyjaszewski, *Macromolecules* **2017**, *50*, 2942–2950; b) J. A. Hanson, C. B. Chang, S. M. Graves, Z. Li, T. G. Mason, T. J. Deming, *Nature* **2008**, *455*, 85–88; c) W. Li, Y. Yu, M. Lamson, M. S. Silverstein, R. D. Tilton, K. Matyjaszewski, *Macromolecules* **2012**, *45*, 9419–9426.

[3] H. C. Shum, Y. J. Zhao, S. H. Kim, D. A. Weitz, *Angew. Chem. Int. Ed.* **2011**, *50*, 1648–1651; *Angew. Chem.* **2011**, *123*, 1686–1689.

[4] Y. Jiang, R. Chakroun, P. Gu, A. H. Groschel, T. P. Russell, *Angew. Chem. Int. Ed.* **2020**, *59*, 12751–12755; *Angew. Chem.* **2020**, *132*, 12851–12855.

[5] a) J. Zhao, Z. Pan, D. Snyder, H. A. Stone, T. Emrick, *J. Am. Chem. Soc.* **2021**, *143*, 5558–5564; b) K. H. Ku, J. M. Shin, D.

Klinger, S. G. Jang, R. C. Hayward, C. J. Hawker, B. J. Kim, *ACS Nano* **2016**, *10*, 5243–5251.
[6] a) J. Bae, T. P. Russell, R. C. Hayward, *Angew. Chem. Int. Ed.* **2014**, *53*, 8240–8245; *Angew. Chem.* **2014**, *126*, 8379–8384; b) Y. Chai, A. Lukito, Y. Jiang, P. D. Ashby, T. P. Russell, *Nano Lett.* **2017**, *17*, 6453–6457; c) Q. Chen, Y. Xu, X. Cao, L. Qin, Z. An, *Polym. Chem.* **2014**, *5*, 175–185; d) D. J. French, J. Fowler, P. Taylor, P. S. Clegg, *Soft Matter* **2020**, *16*, 7342–7349.
[7] a) A. Salonen, D. Langevin, P. Perrin, *Soft Matter* **2010**, *6*, 0■■please provide DOI or page numbers!■■; b) J. Lee, K. H. Ku, J. Kim, Y. J. Lee, S. G. Jang, B. J. Kim, *J. Am. Chem. Soc.* **2019**, *141*, 15348–15355.
[8] R. H. Staff, M. Gallei, M. Mazurowski, M. Rehahn, R. Berger, K. Landfester, D. Crespy, *ACS Nano* **2012**, *6*, 9042–9049.
[9] a) M. J. T. Raaijmakers, N. E. Benes, *Prog. Polym. Sci.* **2016**, *63*, 86–142; b) K. Piradashvili, E. M. Alexandrino, F. R. Wurm, K. Landfester, *Chem. Rev.* **2016**, *116*, 2141–2169; c) Z. Niu, J. He, T. P. Russell, Q. Wang, *Angew. Chem. Int. Ed.* **2010**, *49*, 10052–10066; *Angew. Chem.* **2010**, *122*, 10250–10265.
[10] a) D. M. Yu, D. M. Smith, H. Kim, J. Rzayev, T. P. Russell, *Macromolecules* **2019**, *52*, 6458–6466; b) D. M. Yu, D. M. Smith, H. Kim, J. K. D. Mapas, J. Rzayev, T. P. Russell, *Macromolecules* **2019**, *52*, 3592–3600; c) D. M. Yu, J. K. D. Mapas, H. Kim, J. Choi, A. E. Ribbe, J. Rzayev, T. P. Russell, *Macromolecules* **2018**, *51*, 1031–1040; d) G. Jeong, D. M. Yu, J. K. D. Mapas, Z. Sun, J. Rzayev, T. P. Russell, *Macromolecules* **2017**, *50*, 7148–7154; e) M. Hu, X. Li, J. Rzayev, T. P. Russell, *Macromolecules* **2021**, *54*, 0■■please provide DOI or page numbers!■■.
[11] a) Y. Lin, A. Boker, H. Skaff, D. Cookson, A. D. Dinsmore, T. Emrick, T. P. Russell, *Langmuir* **2005**, *21*, 191–194; b) B. Frank, A. P. Gast, T. P. Russell, H. R. Brown, C. Hawker, *Macromolecules* **1996**, *29*, 6531–6534; c) D. Axelrod, D. E. Koppel, J. Schlessinger, E. Elson, W. W. Webb, *Biophys. J.* **1976**, *16*, 1055–1069.
[12] D. M. Barber, Z. Yang, L. Prévost, O. du Roure, A. Lindner, T. Emrick, A. J. Crosby, *Adv. Funct. Mater.* **2020**, *30*, 2002704.
[13] K. Du, E. Glogowski, T. Emrick, T. P. Russell, A. D. Dinsmore, *Langmuir* **2010**, *26*, 12518–12522.
[14] L. P. Ozorio, R. Pianzolli, M. B. S. Mota, C. J. A. Mota, *J. Braz. Chem. Soc.* **2012**, *23*, 931–937.
[15] a) T. P. Russell, G. Coulon, V. R. Deline, D. C. Miller, *Macromolecules* **1989**, *22*, 4600–4606; b) G. Coulon, T. P. Russell, V. R. Deline, P. F. Green, *Macromolecules* **1989**, *22*, 2581–2589.
[16] M. M. Martin, L. Lindqvist, *J. Lumin.* **1975**, *10*, 381–390.

Manuscript received: January 25, 2022
Accepted manuscript online: April 6, 2022
Version of record online: ■■, ■■

Research Articles

Interfaces

Z. Chen, M. Hu, X. Li, D. Smith, H.-G. Seong, T. Emrick, J. Rzayev,* T. P. Russell* _____ e202201392

In Situ Hydrolysis of Block Copolymers at the Water-Oil Interface

Real-time pendant drop tensiometry of a toluene solution of poly(solketal methacrylate-*b*-styrene) (PSM-*b*-PS) in water to monitor the conversion of PSM blocks into glycerol monomethacrylate (GM) blocks upon the addition of acid to the aqueous phase. This work provides opportunities to quantitatively monitor the responsive block copolymers for structured liquids.

@UMassPSE

Share your work on social media! *Angewandte Chemie* has added Twitter as a means to promote your article. Twitter is an online microblogging service that enables its users to send and read short messages and media, known as tweets. Please check the pre-written tweet in the galley proofs for accuracy. If you, your team, or institution have a Twitter account, please include its handle @username. Please use hashtags only for the most important keywords, such as #catalysis, #nanoparticles, or #proteindesign. The ToC picture and a link to your article will be added automatically, so the **tweet text must not exceed 250 characters**. This tweet will be posted on the journal's Twitter account (follow us @ange_chem) upon publication of your article in its final (possibly unpaginated) form. We recommend you to re-tweet it to alert more researchers about your publication, or to point it out to your institution's social media team.

Please check that the ORCID identifiers listed below are correct. We encourage all authors to provide an ORCID identifier for each coauthor. ORCID is a registry that provides researchers with a unique digital identifier. Some funding agencies recommend or even require the inclusion of ORCID IDs in all published articles, and authors should consult their funding agency guidelines for details. Registration is easy and free; for further information, see http://orcid.org/.

Zhan Chen
Mingqiu Hu
Xindi Li
Darren Smith
Hong-Gyu Seong
Prof. Todd Emrick http://orcid.org/0000-0003-0460-1797
Prof. Javid Rzayev http://orcid.org/0000-0002-9280-1811
Prof. Thomas P. Russell http://orcid.org/0000-0001-6384-5826